Contents lists available at ScienceDirect

EBioMedicine

Up-regulated FHL2 inhibits ovulation through interacting with androgen receptor and ERK1/2 in polycystic ovary syndrome

Ruiqiong Zhou[a,b], Shang Li[a,b], Jiansheng Liu[a,b], Hasiximuke Wu[a,b], Guangxin Yao[a,b], Yun Sun[a,b], Zi-Jiang Chen[a,b,c], Weiping Li[a,b], Yanzhi Du[a,b,*]

[a] Center for Reproductive Medicine, Ren Ji Hospital, School of Medicine, Shanghai Jiao Tong University, Shanghai 200135, China
[b] Shanghai Key Laboratory for Assisted Reproduction and Reproductive Genetics, Shanghai 200135, China
[c] National Research Center for Assisted Reproductive Technology and Reproductive Genetics, The Key Laboratory for Reproductive Endocrinology of Ministry of Education, Shandong Provincial Key Laboratory of Reproductive Medicine, Center for Reproductive Medicine, Shandong Provincial Hospital, Shandong University, Jinan 250021, China

A R T I C L E   I N F O

A B S T R A C T

Background: The ovulatory dysfunction mechanisms underlying polycystic ovary syndrome (PCOS) are not completely understood. There is no effective therapy for PCOS so far.

Methods: We measured the expression of four and a half LIM domain 2 (FHL2) and other related-genes in human granulosa cells (hGCs) from patients with and without PCOS. To minimise the heterogeneity of patients with PCOS, we only included PCOS patients meeting all three criteria according to the revised Rotterdam consensus. The *in vitro* effects of FHL2 on ovulatory genes and the underlying mechanisms were examined in KGN cells. The role of FHL2 in ovulation was investigated *in vivo* by overexpressing FHL2 in rat ovaries via intrabursal lentivirus injection.

Findings: Increased FHL2 and androgen receptor (AR) expression and decreased CCAAT/enhancer-binding protein β (C/EBPβ) expression were observed in hGCs from patients with PCOS. FHL2 inhibited the expression of ovulation-related genes, including phosphorylated ERK1/2, C/EBPβ, COX2 and HAS2 in KGN cells. It was partially by interacting with AR to act as its co-regulator to inhibit C/EBPβ expression and by binding to ERK1/2 to inhibit its phosphorylation. Moreover, FHL2 abundance in hGCs was positively correlated with the basal serum testosterone concentration of patients with PCOS, and dihydrotestosterone (DHT)-induced FHL2 upregulation was mediated by AR signalling in KGN cells. Additionally, lentiviral-mediated functional FHL2 overexpression in rat ovaries for 1 week contributed to an impaired superovulatory response, displaying decreased numbers of retrieved oocytes and a lower MII oocyte rate. 3-week FHL2 overexpression rat models without superovulation led to acyclicity and polycystic ovary morphology.

Interpretation: Our findings provide novel insights into the mechanisms underlying the pathogenesis of PCOS, suggesting that FHL2 could be a potential treatment target for ovulatory obstacles in PCOS.

Fund: National Key Research and Development Program of China, National Natural Science Foundation, National Institutes of Health project and Shanghai Commission of Science and Technology.

1. Introduction

Polycystic ovary syndrome (PCOS) is one of the most common endocrine and metabolic disorders in premenopausal women, and it affects 5%–20% of women of reproductive age worldwide [1]. PCOS is a complicated syndrome, and its cause is implicated genetic, epigenetic and environmental factors in the pathophysiology of PCOS [2]. Heterogeneous by nature, this condition is characterised by hyperandrogenism, ovulatory dysfunction and polycystic ovarian morphology (PCOM), with excessive androgen production by ovaries being a key feature [3–5]. PCOS accounts for more than 75% cases of anovulatory infertility [6] which is caused by follicular arrest and ovulatory dysfunction [7,8]. Despite intensive research, the mechanisms underlying aberrant follicular development and anovulation in PCOS remain largely obscure.

Ovulation is triggered when the ovulatory surge of luteinising hormone (LH) activates the LH/CG receptor in the mural granulosa cells (GCs) of the preovulatory follicle. This initial signal is propagated to the cumulus cells and oocytes through paracrine and autocrine

* Corresponding author at: 845 Lingshan Road, Shanghai 200135, China.
E-mail address: duyz@sjtu.edu.cn (Y. Du).

Research in context

Evidence before this study

Polycystic ovary syndrome (PCOS) is a complex endocrine condition characterised by oligo-ovulation/anovulation, hyperandrogenism, and polycystic ovarian morphology. The ovulatory dysfunction mechanisms underlying PCOS are not completely understood. Ovulation is a complicated process influenced by multiple factors. The essential role of the ERK signalling cascade has been demonstrated with substantial evidence that it regulates all three steps of the ovulation: resumption of meiosis, expansion of cumulus cells, and follicular rupture. CCAAT/enhancer-binding protein β (C/EBPβ) is an essential extracellular signal-regulated kinase (ERK) 1/2-mediated ovulatory gene, and its lower expression in human granulosa cells (hGCs) from patients with PCOS was recently demonstrated by our laboratory. Published microarray data suggest that four and a half LIM domain 2 (FHL2) may be related to C/EBPβ-regulated genes in PCOS. The FHL proteins are structurally composed of four LIM domains and an N-terminal half LIM domain that do not bind to DNA; instead, they are important mediators of protein—protein interactions, with each member displaying tissue-specific developmental and organ-specific expression patterns. FHL2 is expressed in the heart, gonads, prostate, adrenal gland, and intestines, serving as a transcriptional regulator through its interaction with various transcription factors. It has been reported that FHL2 binds to androgen receptor (AR) and modulates its transcriptional activity in prostate cancer, whereas mounting evidence indicates that AR-mediated actions are strongly implicated in the development of PCOS. Meanwhile, FHL2 functions as a negative regulator of MAPK/ERK signalling in cardiomyocytes. FHL2 knockout mice are viable, but their reproductive function has not been carefully examined. FHL2 expression has been detected in the ovaries; however, its function in the reproductive system remains largely unknown. Hence, we considered whether FHL2 can act as a co-regulator with pivotal transcription factors that are involved in the pathogenesis of PCOS. To the best of our knowledge, no study has demonstrated the role for FHL2 in female reproductive diseases. The correlation between FHL2 and ovulation remains unclear and needs to be investigated.

Added value of this study

Our study demonstrated that FHL2 may play a role in the ovulatory disorder of PCOS. Increased abundance of FHL2 and AR as well as decreased abundance of C/EBPβ were detected in hGCs from patients with PCOS, thereby we explored the underlying molecular mechanisms *in vitro* experiments on KGN cells. First, FHL2 acts as a coregulator of AR via protein—protein interactions to inhibit the expression of C/EBPβ, which could further repress its downstream ovulatory genes. Second, FHL2 functions as a negative upstream regulator of ERK signalling pathways to inhibit ovulation. Moreover, we found that FHL2 expression in hGCs was positively correlated with basal testosterone levels in patients with PCOS, and DHT-induced upregulation of FHL2 is mediated by AR signalling. Then, we conducted *in vivo* gain-of-function studies in rat ovaries to identify the role of FHL2 in ovulation. One week of lentiviral-mediated functional FHL2 overexpression in rat ovaries followed by superovulation resulted in decreased numbers of retrieved oocytes and a lower MII oocyte rate, and 3-week rat models without superovulation led to acyclicity and polycystic ovary morphology.

Implications of all the available evidence

Our findings provide novel insights into the mechanisms underlying the pathogenesis of PCOS; in particular, FHL2 may be involved in the development of ovarian features of PCOS, and inhibition of FHL2 in combination with assisted reproductive technology could be a potential therapeutic approach for ovulatory dysfunction in PCOS.

signalling pathways, resulting in the release of a fertilisable oocyte [9]. This process is divided into three discreet steps: resumption of meiosis, expansion of cumulus cells, and follicular rupture. Substantial evidence indicates the essential role of the epidermal growth factor receptor/extracellular signal-regulated kinase (ERK) 1/2 signalling cascade in ovulation [10−13]. Mice with genetic inactivation of the ERK1/2 cascade in GCs are sterile, and remarkably, oocyte meiotic maturation, cumulus expansion, and follicle rupture are completely abolished [14]. Previous microarray analyses revealed that ERK1/2 depletion alters the expression of 77% of LH-regulated genes [14]. The transcription factor CCAAT/enhancer-binding protein β (C/EBPβ) is induced and phosphorylated in response to the LH surge in an ERK1/2-sensitive manner [14,15], and it mediates some of the effects of ERK1/2 on the ovaries [15].

The abnormal gene expression profiles of GCs and ovaries from patients with PCOS have revealed many differentially expressed genes [16−18]. Using bioinformatics methods (DAVID Bioinformatics Resources 6.7), we screened for genes which can regulate the differentially expressed genes in PCOS based on published microarray data [16−18]. Among these regulatory genes, four and a half LIM domain (FHL) 1 and 2 as well as C/EBPβ were identified based on the high frequencies of their occurrence in the gene expression profiles. C/EBPβ is an essential ERK1/2-mediated ovulation-related gene [15], and its lower expression in hGCs from patients with PCOS that involved in the pathogenesis of ovulatory dysfunction of PCOS has been demonstrated by our research group [19]. Therefore, we hypothesised that FHL1/2 plays a role in the development of PCOS and we examined whether FHL1/2 can regulate ovulation-related genes related to ovulatory disorder in PCOS. Because we found no difference of FHL1 abundance in hGCs between patients with and those without PCOS, we focused on the role of FHL2 in the development of PCOS in the current study.

FHL proteins are structurally composed of four LIM domains and an N-terminal half LIM domain, and they do not bind to DNA. Instead, they are important mediators of protein—protein interactions [20]. The FHL family of multifunctional proteins is composed of five members (FHL1−4 and activator of cAMP responsive element modulator in the testes), with each gene displaying tissue specific developmental and organ-specific expression patterns [21]. FHL2 is expressed in the heart, gonads, prostate, adrenal gland, and intestines [22−24], and it can regulate the transcription of genes involved in cell proliferation and tumorigenesis [23,25−27], bone formation [28,29], and cardiac function [30−32] by serving as a transcriptional regulator through its interaction with various transcription factors. FHL2 expression has been detected in the ovaries [22,33], and it can act as a transcriptional coactivator of NR5A family and CREB to activate the inhibin-α gene in mouse ovarian granulosa cells, however, its function in reproduction remains largely unknown.

Hyperandrogenism, the most consistent feature of PCOS [34], is implicated as a key mediator of the pathogenesis of PCOS. As all direct androgen actions are mediated by AR, AR-mediated actions are thereby implicated in the development of PCOS [35,36]; however, its downstream underlying mechanisms remain unclear. FHL2 reportedly binds to AR and modulates its transcriptional activity in prostate cancer [37,38], and another study suggests that AR activity could suppress the expression of C/EBPβ, a direct AR transcriptional repression target in prostate cancer cells [39].

To the best of our knowledge, no study has provided evidence that FHL2 plays a role in female reproductive diseases. In this study, we found that the abundance of FHL2 and AR was remarkably higher in hGCs from patients with PCOS, whereas that of C/EBPβ was lower.

FHL2 overexpression inhibited ovulation-related genes *in vitro* and *in vivo*, partially by interacting with AR by acting as its co-repressor to suppress the expression of C/EBPβ and by binding to ERK1/2 to inhibit its phosphorylation, inducing further suppression of other ovulation-related genes. Moreover, we found that androgen effects on upregulation of FHL2 may be partially mediated by AR. Our data provide insights into the potential of FHL2 inhibition as a therapeutic approach for targeting AR-mediated androgen actions and ERK signalling to tackle ovulatory dysfunction in PCOS.

2. Materials and methods

2.1. Human subjects and GC samples

The study participants included women undergoing *in vitro* fertilisation-embryo transfer (IVF-ET) at the centre for Reproductive Medicine, Ren Ji Hospital, Shanghai Jiao Tong University School of Medicine. Appropriate informed consent was obtained from all patients in this study. To minimise the heterogeneity of patients with PCOS, 37 patients meeting all three criteria (oligo-ovulation and/or anovulation, hyperandrogenism, and PCOM) according to the revised Rotterdam consensus [40] were recruited into the PCOS group, and 33 patients without PCOS (non-PCOS group) were selected because of tubal and/or male factor infertility with regular menstrual cycles and normal ovarian morphologies. All subjects (20−35 years old) were of Han ethnicity, and they did not receive hormonal therapy at least 3 months before the study. Clinical information of the patients is presented in Table 1. All patients underwent a gonadotropin-releasing hormone antagonist protocol with a human chorionic gonadotropin (hCG) trigger. Upon oocyte retrieval, follicular fluid was collected from size-matched dominant follicles (18−20 mm), and GCs in the follicular fluid were pelleted followed by purification with the Ficoll-Paque (GE Healthcare Bio-Sciences, NJ, USA) density centrifugation. After digestion with hyaluronidase (Sigma, Chemical Co., St Louis, MO, USA), cells from a single subject were used for RNA extraction without culture, and cells from three or four normal subjects were pooled for culture in Dulbecco's modified Eagle's medium/Ham's F12 (DMEM/F12) (Gibco, Grand Island, NY, USA) containing 10% charcoal-stripped foetal bovine serum (FBS) (Gibco) and antibiotics (Invitrogen, CA, USA). The Institutional Review Board of the Ren Ji Hospital, School of Medicine, Shanghai Jiao Tong University, reviewed and approved all procedures.

2.2. Cell culture

KGN cells were kindly provided by the centre of Reproductive Medicine, Shandong Provincial Hospital. The cells were cultured in phenol red-free DMEM/F12 (Gibco) containing 10% charcoal-stripped FBS and antibiotics and incubated at 37 °C in a humidified atmosphere containing 5% CO2. KGN cells were routinely passaged every 2−3 days.

2.3. Cell treatment

For hCG stimulation, hGCs were retrieved from follicular fluid as previously described, and 3 days after plating, the cells were treated with hCG (10 IU/ml; Lizhu, Zhuhai, China) according to a previous study [41]. The incubation time for each study is given in the corresponding figures.

Forskolin (FSK, 10 μM; R&D Systems, Minnesota, USA) was used to mimic the effect of the LH surge [15,42,43] to activate PKA signalling pathway in KGN cells. The incubation time for each study is given in the corresponding figures. To inhibit ERK signalling, the cells were pre-treated with U0126 (10 μM, a MEK1/2 inhibitor; Selleckchem, Houston, TX, USA) for 1 h followed by FSK for 4 h.

For androgen stimulation, we used dihydrotestosterone (DHT) (Sigma-Aldrich) to activate AR activity [44]. To determine the working level of DHT, we examined the effects of various concentrations of DHT on the induction of AR and FHL2 expression. To inhibit AR signalling, KGN cells were pre-incubated with flutamide (5 μM, an androgen receptor inhibitor; Sigma-Aldrich) for 24 h followed by incubation with DHT for 24 h.

2.4. Immunofluorescence staining

After treatment with FSK for 4 h, KGN cells were fixed in a chamber slide (Millipore, Billerica, USA) in 4% paraformaldehyde and then permeabilised with 0.4% Triton X-100. After washing, the cells were blocked with normal goat serum (Proteintech, Wuhan, China) for 1 h and then incubated with FHL2 antibody (1:50; Proteintech) overnight at 4 °C. After washing, Alexa Fluor 594-conjugated anti-mouse IgG (green) (1:200; Proteintech) was used as the secondary antibody, and the cells were incubated in the dark for 2 h. The nuclei were counterstained with 4′,6-diamidino-2-phenylindole (DAPI) (blue). Cells were observed and imaged using a fluorescence microscope (Zeiss, Oberkochen, Germany).

Three days after plating, same method of immunofluorescence staining was used in hGCs after treatment with hCG (10 IU/ml, 4 h).

2.5. Transfection of small interfering RNA (siRNA)

KGN cells (2 × 10⁵) were seeded into 6-well plates, cultured for 1 day and then transfected with siRNAs using the Lipofectamine 3000 Reagent (Invitrogen) according to the manufacturer's protocol. After transfection, the cells were incubated for 48 h before further treatment. The specific sequences of target genes were as follows:

FHL2 siRNA-1, 5′-CCUGCUAUGAGAAACAACATT-3′;

FHL2 siRNA-2, 5′- GCAAGGACUUGUCUUACAATT-3′;

AR siRNA, 5′-GAAAUGAUUGCACUAUUGAUU-3′;

C/EBPβ siRNA, 5′-GCACCCUGCGGAACUUGUUTT-3′; and

non-specific scrambled siRNA, 5′-UUCUCCGAACGUGUCACGUTT-3′.

2.6. Establishment of stable transfected KGN cells with exogenous FHL2 lentivirus vectors and control vectors

KGN cells were cultured till a confluence of 30%−40% was achieved and then transfected with lentivirus-mediated human FHL2 overexpression vectors (LV-FHL2[25555-1]) or control vectors

Table 1
Demographic features of recruited subjects with and without PCOS.

Clinical parameter	Non-PCOS	PCOS
No.	33	37
Age (y)	28.37 ± 3.22	28.83 ± 2.64
BMI (kg/m²)	21.66 ± 2.48	23.56 ± 3.22*
AFC	11.97 ± 2.76	22.83 ± 11.72*
Basal FSH (mIU/ml)	6.29 ± 1.32	6.28 ± 1.13
Basal LH (mIU/ml)	5.04 ± 2.89	9.97 ± 6.31*
Basal E₂ (pg/ml)	36.93 ± 17.26	36.57 ± 35.01
Basal T (nmol/l)	0.88 ± 0.39	1.55 ± 0.87*
AMH (ng/ml)	4.89 ± 1.91	11.97 ± 4.66*
Fasting glucose (mmol/ml)	5.24 ± 0.52	5.09 ± 0.51
Fasting insulin (IU/ml)	7.13 ± 2.47	11.20 ± 4.10*

Data are mean ± SD values.
*$P < 0.05$ vs. Non-PCOS.
BMI: body mass index; AFC: basal antral follicle count; FSH: follicle-stimulating hormone; LH: luteinizing hormone; E2: Oestradiol; T: testosterone; AMH: anti-mullerian hormone.

(CON335), which were purchased from GeneChem Company (Shanghai, China). Two days following transfection, cells were selected with puromycin (5 μg/ml) for 7 days. Stable cell lines were examined for FHL2 expression by quantitative real-time polymerase chain reaction (qRT-PCR), immunoblotting, and green fluorescent protein (GFP) expression after transfection.

For rescue experiments, after establishing stable KGN cell lines carrying lentivirus-mediated FHL2 overexpression or control vectors, cells were transfected with AR siRNA using Lipofectamine 3000 for 48 h before analysis.

2.7. Extraction of RNA for qRT-PCR

Total RNA was extracted from cells using a total RNA extraction kit (Foregene Co., Ltd., Sichuan, China), and mRNA was reverse-transcribed into cDNA using the PrimeScript RT Master Mix Perfect Real-Time kit (TaKaRa, Dalian, China). The target mRNA was measured using qRT-PCR, and GAPDH was amplified in parallel as an internal loading control. The absolute mRNA level in each sample was calculated according to a standard curve created using serial dilutions of known amounts of PCR products against corresponding cycle threshold values. The primer sequences used for PCR are listed in Supplementary Table S1.

2.8. Extraction of protein and analysis via Western blotting

The cells were lysed in ice-cold radioimmunoprecipitation assay lysis buffer (Cell signalling Technology, MA, USA) containing a protease inhibitor cocktail (Roche, Basel, Switzerland) and phosphatase inhibitor (Roche). Protein (40 μg) from each sample was electrophoresed in a 10% sodium dodecyl sulphate−polyacrylamide gel and transferred to a nitrocellulose blot. After blocking, the blot was incubated with antibodies against FHL2 (1:1000; Proteintech), FHL2 (1:1000; Abcam, Cambridge, UK), AR (1:400; Santa Cruz Biotechnology, CA, USA), AR (1:1000; Cell signalling Technology), C/EBPβ (1:400; Santa Cruz Biotechnology), COX2 (1:1000; Proteintech), HAS2 (1:1000; Abcam), total ERK1/2, and ERK1/2 phosphorylated at Thr202/Tyr204 (1:2000; Cell signalling Technology) overnight at 4 °C, followed by incubation with secondary antibodies (1:5000; SAB, Maryland, USA). An enhanced chemiluminescence detection system (Millipore) was used to detect protein bands. The same blot was probed for GAPDH (1:2000; Proteintech) as an internal loading control. The bands were visualised using the G-Box iChemi Chemiluminescence Image Capture System (Syngene, MD, USA).

2.9. Co-immunoprecipitation (co-IP)

Co-IP was performed in lysates prepared from pre-treated KGN cells (150 μg of total protein) using an FHL2 antibody (Proteintech) or normal rabbit IgG (Millipore) overnight at 4 °C with gentle rotation. On the next morning, the protein−antibody complex was incubated with 20 μl of magnetic Protein A+G Beads (Millipore) for 1 h at 4 °C with gentle rotation. Then, the antibody−protein−bead complex was washed five times with co-IP buffer (Cell signalling Technology). Then, the protein in the complex was eluted with 20 μl of 1 × loading buffer and boiled before running on a 10% SDS-polyacrylamide gel and transferred to a nitrocellulose membrane. After blocking, FHL2-combined AR protein or FHL2-combined total ERK1/2 protein was immunoblotted using antibodies against AR or total ERK1/2.

2.10. Chromatin immunoprecipitation (ChIP)

ChIP was performed to examine the binding of AR to the promoter of C/EBPβ. The ChIP experiment was performed using the Magna ChIP^{TM} A/G Kit (Millipore) according to the manufacturer's instructions. An AR antibody (Cell signalling Technology) was used for immunoprecipitation. An equal amount of pre-immune IgG (Proteintech) served as the negative control. The primers amplifying the putative AR-binding site in the C/EBPβ promoter region were as follows: 5′-ACGGAAATGAAGCAGGGGTGT-3′ (forward) and 5′-CACAG-CACGCTCAACATTTACCAG-3′ (reverse). The same amount of sheared DNA without antibody precipitation served as the input control. The ratio of DNA precipitated by the AR antibody over the input control was obtained to indicate the amounts of transcription factors bound to the C/EBPβ promoter.

2.11. Injection of lentivirus-mediated vectors into rat ovaries

All rat experiments were approved by the Institutional Review Board of Ren Ji Hospital, School of Medicine, Shanghai Jiao Tong University. All rats received humane care in accordance with the National Institutes of Health Guide for the Care and Use of Laboratory Animals.

The rat Fhl2 overexpression lentivirus vectors (LV-Fhl2[44,116−1]) and control empty lentiviral vectors (LV-Control[CON238]) (GeneChem) were injected intrabursally into the ovaries of 6-week-old female Sprague−Dawley (SD) rats using a 10-μl microsyringe, and the virus titre was 1 × 108 TU/ml. The construct of LV-Fhl2 was inserted into the Ubi-MCS-3FLAG-SV40-EGFP-IRES-puromycin lentiviral vector (GeneChem, GV358). The negative control was the corresponding empty lentiviral vector. The lentivirus vector protocol was modified from the published method [45−47] and combined with our previous experience [19,48]. In brief, we used 293T cells to confirm the transfection efficiency and determined the proper virus titre by examining the expression of FHL2 using qRT-PCR and immunoblotting. We created a small incision on the back of each side of each rat, separated the ovaries, and slowly injected 10 μl of lentivirus-contained solutions using a microsyringe needle. The needle was carefully held in place for several minutes after the injection. Finally, we sutured the muscle and skin layers. Because the lentiviral vector system contained GFP, we fixed rat ovaries with 4% paraformaldehyde and then embedded them in paraffin. The ovarian sections were directly visualised under a fluorescence microscope (Zeiss) to determine the distribution and efficiency of lentiviral transfection.

2.12. Superovulation

For the first part of the animal study, 38 rats (6 weeks old) were randomly divided into three groups to receive hCG at 0 (n = 10; pregnant mare serum gonadotropin (PMSG) 48 h), 4 (n = 10) or 16 h (n = 18). One week after lentivirus injection, superovulation [49] was induced via the intraperitoneal injection of PMSG (300 IU/kg) at 4 p.m., followed by hCG injection (300 IU/kg) (Sansheng Pharmaceutical, Shanghai, China) after 48 h. The rats were sacrificed by decapitation at the pre-determined time after superovulation. Cumulus−oocyte complexes (COCs) were collected from the oviducts at 16 h after hCG injection. Oocytes were freed from cumulus cells via digestion with 0·1% hyaluronidase (Vitrolife, Frölunda, Sweden) for 5 min. Oocytes which reached the MII stage were recorded, and images were taken using a Zeiss microscope [50].

For the second part of the animal study, 10 rats were randomly divided into two groups and directly sacrificed 3 weeks after the lentivirus injection without superovulation to explore the long-term impact of lentivirus-mediated *Fhl2* overexpression in rat ovaries. We observed the oestrous cycle by examining the vaginal cytology over the last 8 consecutive days.

2.13. Measurement of serum progesterone levels via enzyme-linked immunosorbent assay (ELISA)

Rat blood samples were obtained via cardiac exsanguination under avertin anaesthesia and immediately centrifuged at 2500 rpm for 15 min to obtain serum samples, which were stored at −80 °C.

A progesterone-specific ELISA kit (TSZ, San Francisco, USA) was used to analyse rat serum progesterone levels via ELISA. All procedures were performed according to the manufacturers' standard protocol.

2.14. Histology

Rat ovaries were fixed in 4% paraformaldehyde and then embedded in paraffin. Five μm-thick tissue sections were deparaffinized and rehydrated through a graded ethanol series. The sections were stained with haematoxylin and eosin (HE) and then observed using a microscope (Zeiss). Ovaries were serially sectioned at 20 μm. Total numbers of preantral follicles (oocyte surrounded by 1.5 to 5 layers of granulosa cells), small antral follicles (oocyte surrounded with more than 5 layers of granulosa cells, and/or one or two small areas of follicular fluid), large antral follicles (contained a single large antral cavity), corpora lutea (CL) and cyst-like follicles (large fluid-filled cysts with an attenuated granulosa cell layer, dispersed theca cell layer, and an oocyte lacking connection to the granulosa cells) were classified and quantified as previously reported [51,52]. To avoid repetitive counting, each follicle was only counted in the section where the oocyte's nucleolus was visible. For all large antral follicles, granulosa cell layer thickness and theca layer area were measured using Image J software (version 1.48; NIH).

2.15. Statistical analysis

All data are reported as mean $\pm$ SD or SEM. The Kolmogorov−Smirnov test was used to determine whether continuous variables were normally distributed. A paired or unpaired Student's t-test or one-way analysis of variance followed by the Student−Newman−Keuls multiple comparison test was used where appropriate to assess significant differences. Correlation between the variables was performed using Pearson or Spearman rank correlation analysis according to distributions of relevant variables. Significance was set at P-value of < 0.05. Statistical significance was evaluated using data from at least three independent experiments.

3. Results

3.1. Increased abundance of FHL2 and AR and decreased abundance of C/EBPβ in PCOS

The demographic features of the recruited subjects are summarised in Table 1. Among the 70 recruited subjects, 33 had tubal and/or male factor infertility without PCOS, and 37 had PCOS. Compared with the non-PCOS group, the PCOS group was characterised by increased body mass index and antral follicle count as well as higher basal LH, basal T, AMH, and fasting insulin levels.

As shown in Fig. 1, *FHL2* and *AR* mRNA expression in hGCs was significantly higher in the PCOS group than in the non-PCOS group, whereas there was no difference in terms of *FHL1* mRNA expression

between the two groups. Moreover, *C/EBPβ* abundance was lower in the PCOS group. Therefore, we performed further experiments to explore the mechanism underlying the role of FHL2 in the development of PCOS both *in vitro* and *in vivo*.

3.2. Inhibitory effect of FHL2 on ovulation-related genes in KGN cells

Based on our findings of hGCs from patients with PCOS, we decided to use human granulosa-like KGN cells for *in vitro* experiments to investigate the possible molecular mechanisms underlying FHL2-related pathways in the development of PCOS. siRNA-mediated FHL2 depletion was achieved in KGN cells, and the transfection efficiency was confirmed (Fig. 2a,b). The results illustrated that ovulation-related genes including C/EBPβ, COX2 and HAS2, were significantly upregulated at both mRNA and protein levels following FHL2 depletion (Fig. 2a,b). On the contrary, after establishing FHL2 overexpressing KGN cells and control cells with lentivirus-mediated transfection, the overexpression efficiency was demonstrated at both mRNA and protein levels (Fig. 2c,d), and the ovulation-related genes were evidently impeded in the FHL2-overexpressing KGN cells compared with those in the control cells (Fig. 2c,d). Taken together, these results indicated that FHL2 negatively regulates the expression of ovulation-related genes including C/EBPβ, COX2, and HAS2.

Forskolin (FSK, 10 μM) was used to mimic the LH surge to activate PKA signalling pathway in KGN cells. The results illustrated that treatment with FSK for 4 h, which was a crucial time point for the LH surge to trigger ovulation [10], negatively regulated the mRNA and protein abundance of FHL2 and AR in KGN cells (Fig. 2e,f). Meanwhile, the expression levels of C/EBPβ, COX2 and HAS2 significantly increased after treatment with FSK for 4 h (Fig. 2e,f). Furthermore, treatment with FSK for 4 h effectively increased the mRNA and protein abundance of C/EBPβ, COX2 and HAS2, and FHL2 depletion facilitated the induction of FSK-induced ovulatory genes (Fig. 2g,h). Using cell immunofluorescence, FHL2 staining remarkably decreased after treatment with FSK for 4 h (Fig. 2i). To confirm the effects of FSK-mimicked LH surge on KGN cells, we also cultured hGCs with 10 IU/ml hCG and analysed the expressions of FHL2, AR, C/EBPβ, COX2, and HAS2 at 0, 4, and 16 h after hCG treatment (Fig. S2a,b), which presented similar expression pattern. Meanwhile, an immunofluorescence assay revealed that at 4 h after hCG treatment, FHL2 staining also decreased in hGCs (Fig. S2c). The mechanisms underlying downregulation of FHL2 and AR as well as upregulation of C/EBPβ, COX2 and HAS2 by the LH surge with a similar time pattern remain unknown, suggesting that FHL2 and AR may participate in regulating ovulation.

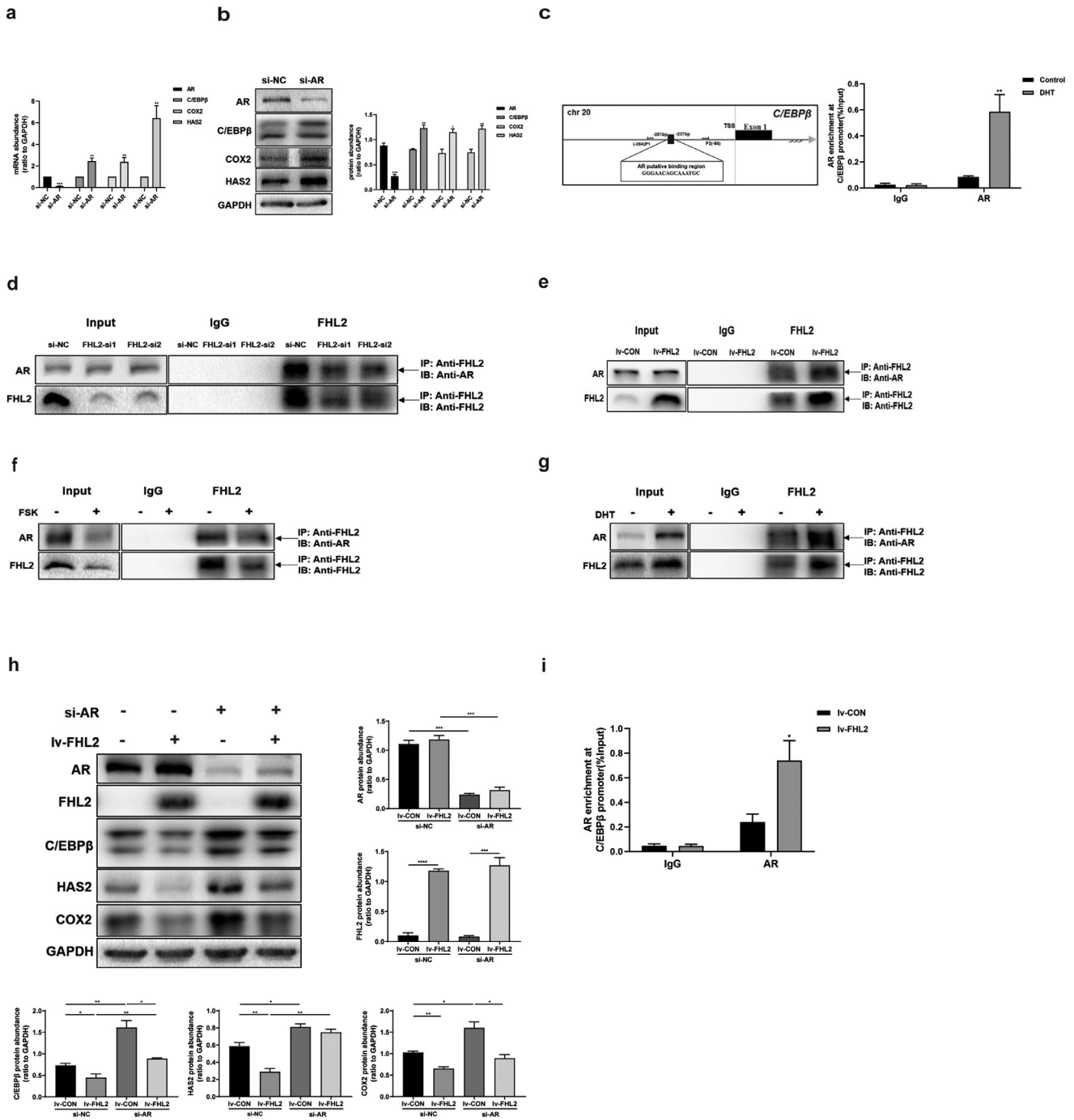### 3.3. FHL2 as a co-repressor of AR to regulate C/EBPβ expression in KGN cells

Based on the fact that AR depletion in KGN cells resulted in increased levels of C/EBPβ, COX2 and HAS2 (Fig. 3a,b), we hypothesised that whether AR can bind to the promoter region of C/EBPβ and
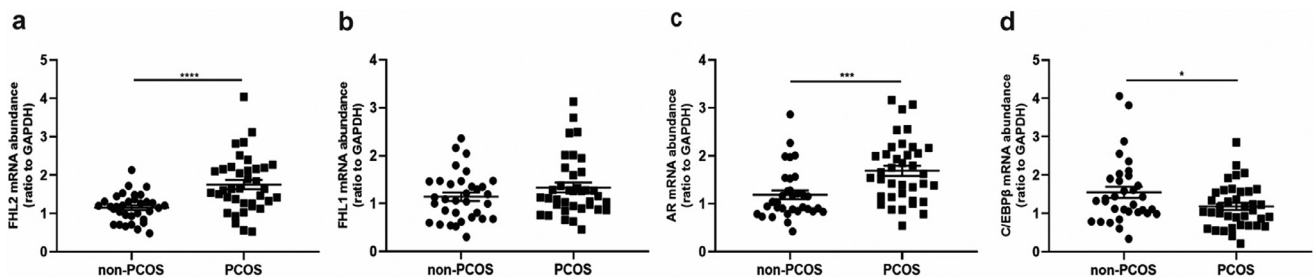
Fig. 1. Increased mRNA expression of FHL2 and AR and decreased C/EBPβ expression in granulosa cells of PCOS patients. Relative mRNA abundance of FHL2 (a), FHL1 (b), AR (c) and C/EBPβ (d) in human granulosa cells (hGCs) from non-PCOS patients (n = 33) and PCOS patients (n = 37) analysed by qRT-PCR. GAPDH values were used for normalization. $^{*}P < 0.05$, $^{***}P < 0.001$, $^{****}P < 0.0001$ vs. non-PCOS patients.
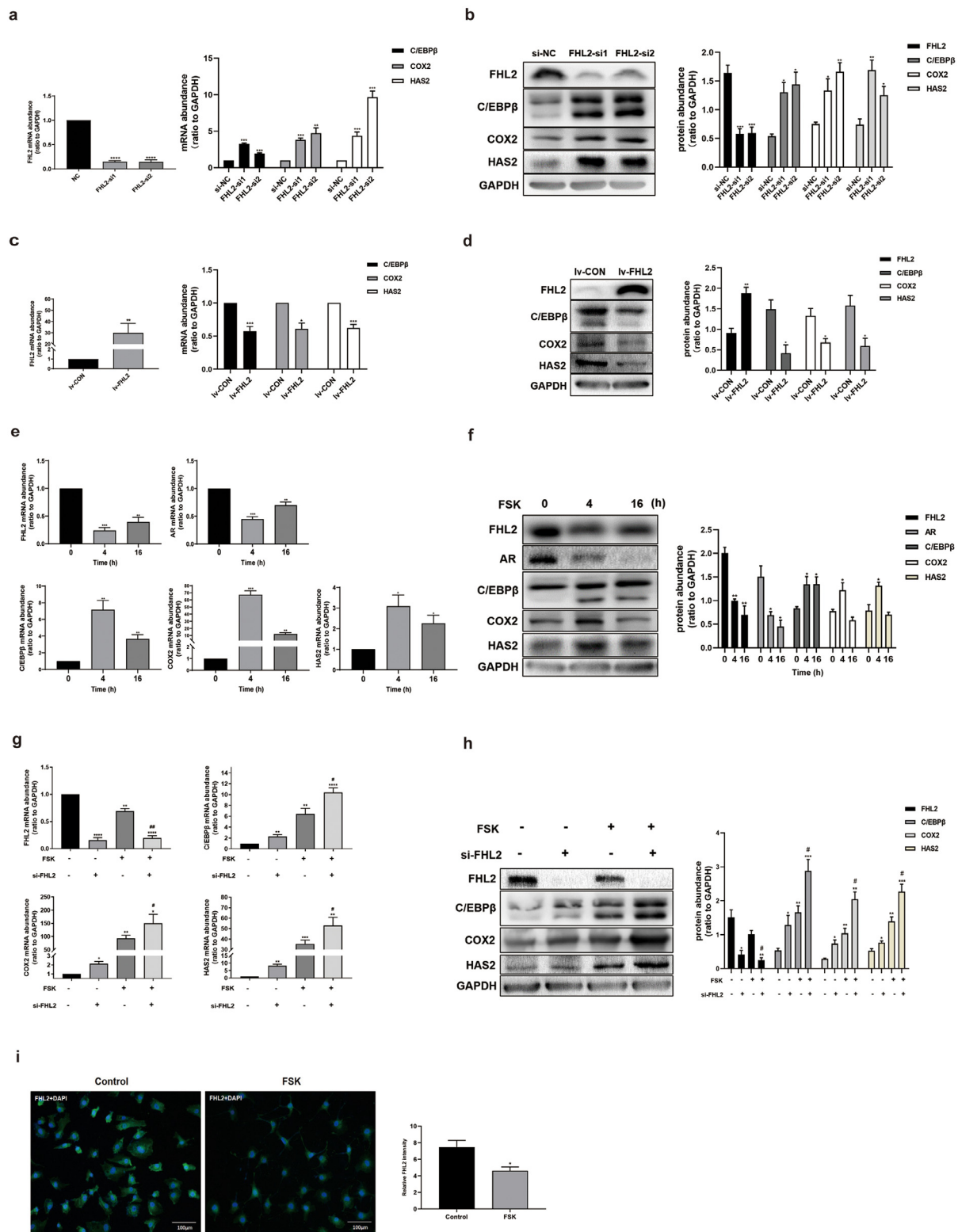
Fig. 2. FHL2 inhibited ovulation-related genes in KGN cells. (a) mRNA abundance of FHL2, C/EBPβ, COX2 and HAS2 after siRNA-mediated FHL2 knockdown in KGN cells detected by qRT-PCR analysis. (b) Protein levels of FHL2, C/EBPβ, COX2 and HAS2 after siRNA-mediated FHL2 knockdown in KGN cells detected by western blot analysis. (c) mRNA abundance of FHL2, C/EBPβ, COX2 and HAS2 after stable transfection of KGN cells mediated by exogenous FHL2 lentivirus vectors or control vectors. (d) Protein abundance of FHL2, C/EBPβ, COX2 and HAS2 after stable transfection of KGN cells mediated by exogenous FHL2 lentivirus vectors or control vectors. (e) Time course effects of Forskolin (FSK, 10 μM) on mRNA levels of FHL2, AR, C/EBPβ, COX2 and HAS2 in KGN cells. (f) Time course effects of Forskolin (FSK, 10 μM) on protein levels of FHL2, AR, C/EBPβ, COX2 and HAS2 in KGN cells. (g) Effects of FSK (10 μM, 4 h) on mRNA levels of FHL2, C/EBPβ, COX2 and HAS2 in the presence and absence of siRNA-mediated knockdown of FHL2 in KGN cells. (h) Effects of FSK (10 μM, 4 h) on protein levels of FHL2, C/EBPβ, COX2 and HAS2 in the presence and absence of siRNA-mediated knockdown of FHL2 in KGN cells. (i) KGN cells treated with FSK (10 μM) for 4 h were fixed and labelled with anti-FHL2 antibodies (green). Cellular nuclei were stained with 4′,6-diamidino-2-phenylindole (DAPI) (blue). The photomicrographs are representative of three independent experiments. Relative fluorescence intensity was analysed using ImageJ software. Representative blots are shown and the data are means ± SEM from 3 to 5 experiments. $^*P < 0.05$, $^{**}P < 0.01$, $^{***}P < 0.001$, $^{****}P < 0.0001$ vs. controls; $^\#P < 0.05$, $^{\#\#}P < 0.01$ vs. FSK. (For interpretation of the references to color in this figure legend, the reader is referred to the web version of this article.)

Fig. 3. FHL2 as a corepressor of AR to inhibit C/EBPβ expression by interacting with AR in KGN cells. (a) Effects of siRNA-mediated AR knockdown on mRNA abundance of AR, C/EBPβ, COX2 and HAS2. (b) Effects of siRNA-mediated AR knockdown on protein levels of AR, C/EBPβ, COX2 and HAS2. (c) The diagram shows the putative binding sites of AR in the C/EBPβ promoter region. TSS, transcription start site. ChIP assays detected the enrichment of AR at the C/EBPβ promoter in response to DHT (10 nM, 24 h) treatment in KGN cells. IgG served as the negative control. (d) With siRNA-mediated FHL2 knockdown, the FHL2-AR interaction was examined in KGN cells by immunoprecipitation of FHL2 from whole-cell lysates followed by immunoblotting for AR and FHL2. About 5% of cell lysis used for co-IP was loaded as inputs. IgG IP was used as control. (e) FHL2-AR interaction was examined in KGN cells by co-IP after stable transfection of KGN cells mediated by exogenous FHL2 lentivirus vectors or control vectors. (f) Effect of FSK (10 μM, 4 h) on FHL2-AR interaction examined by co-IP. (g) Effect of DHT (10 nM, 24 h) on FHL2-AR interaction detected by co-IP. (h) Stable transfection of KGN cells mediated by FHL2 lentivirus vectors or control vectors, followed by siRNA-mediated AR knockdown or nonspecific scrambled siRNA for 48 h before analysis. The protein levels of AR, FHL2, C/EBPβ, HAS2 and COX2 were examined by western blot analysis. (i) ChIP assays detected the enrichment of AR at the C/EBPβ promoter in response to FHL2 overexpression in KGN cells by lentivirus-mediated stable transfection, both control cells and FHL2-overexpressing cells after stable transfection followed by DHT (10 nM, 24 h) before analysis. IgG served as the negative control. Representative blots are shown and the data are means ± SEM from 3 to 5 experiments. *P < 0.05, **P < 0.01, ***P < 0.001, ****P < 0.0001.

repress its transcription. Bioinformatics analysis of the C/EBPβ promoter revealed binding sites for AR spanning the region between −251 and −237 bp (Fig. 3c). KGN cells were cultured with or without DHT (10 nM) for 24 h, and ChIP illustrated that DHT increased the enrichment of AR in this region of the C/EBPβ promoter (Fig. 3c),

suggesting that AR inhibited C/EBPβ expression by binding to its promoter to suppress its transcription. Since FHL2 does not bind to DNA, we considered FHL2 may act as a transcriptional co-regulator of AR. Co-IP demonstrated that FHL2 depletion reduced the interaction between FHL2 and AR; meanwhile, FHL2 overexpression

increased the interaction between FHL2 and AR (Fig. 3d,e). We also detected that after treatment with FSK for 4 h, the interaction between FHL2 and AR decreased, whereas their interaction increased by DHT for 24 h (Fig. 3f,g). These results indicate that FHL2 may inhibit ovulation-related genes by interacting with AR, and LH surge may inhibit their interaction, whereas DHT can enhance their interaction.

Next, we conducted rescue assays to further confirm whether AR is involved in FHL2-induced downregulation of C/EBPβ. FHL2-overexpressing KGN cells exhibited significantly decreased expression of C/EBPβ, COX2 and HAS2, whereas AR depletion prominently increased their expression (Fig. 3h). In addition, FHL2 overexpression−induced downregulation of C/EBPβ and HAS2 was rescued by AR depletion in KGN cells (Fig. 3h). Furthermore, using ChIP, we demonstrated that FHL2-overexpressing KGN cells displayed higher binding of AR to the C/EBPβ promoter than control cells, both following treatment with DHT for 24 h (Fig. 3i). Taken together, these data suggest that FHL2 can function as a co-repressor of AR to inhibit C/EBPβ expression in KGN cells.

3.4. FHL2 as a repressor of ERK1/2 and the role of ERK signalling in regulation of ovulatory genes

To investigate the role of FHL2 on ERK signalling pathway, we found that siRNA-mediated FHL2 depletion significantly increased the phosphorylation of ERK1/2, whereas FHL2-overexpressing KGN cells exhibited lower levels of phosphorylated ERK1/2 than control cells (Fig. 4a,b). Moreover, ERK1/2 phosphorylation increased by treatment with FSK for 4 h in KGN cells (Fig. 4c), similarly, at 4 h after hCG treatment, ERK1/2 phosphorylation increased in hGCs (Fig. S2b). Consistently, FHL2 depletion increased the basal levels of phosphorylated ERK1/2 and further enhanced FSK-induced ERK1/2 phosphorylation (Fig. 4d). To further verify the importance of ERK signalling in regulating ovulation-related genes, we pre-treated cells with U0126 (an inhibitor of MEK, 10 μM) for 1 h and then re-incubated the cells with FSK for 4 h. The results demonstrated that pre-treatment with U0126 effectively abolished the FSK-mimicked LH surge-induced upregulation of C/EBPβ, COX2, and HAS2 (Fig. 4e). These data indicate that the MEK/ERK pathway is engaged further downstream along the PKA signalling pathway activated by LH surge.

To further investigate the mechanism underlying the inhibition of ERK1/2 phosphorylation by FHL2, using co-IP, we found that the depletion of FHL2 decreased the binding between FHL2 and ERK1/2; Meanwhile, FHL2 overexpression increased the interaction between FHL2 and ERK1/2 (Fig. 4f,g). Moreover, cells treated with FSK for 4 h exhibited decreased binding between FHL2 and ERK1/2 (Fig. 4h). These data suggest that FHL2 may inhibit ovulation-related genes by suppressing the phosphorylation of ERK1/2 via interacting with ERK1/2, and LH surge may inhibit their interaction.

3.5. DHT-induced upregulation of FHL2 is mediated by AR

We analysed the correlation between clinical characteristics and the abundance of FHL2 in patients with PCOS (37 samples), in whom FHL2 was positively correlated with the basal T level (Fig. 5a), but no significant correlations were observed between the abundance of FHL2 and other clinical characteristics (data not shown). We used DHT to determine whether androgen stimulation can enhance the expression of FHL2 in vitro. KGN cells were treated with various concentrations of DHT for 24 h, and DHT at the level of 10 nM increased both mRNA and protein levels of FHL2 and AR (Fig. 5b,c,d). Accordingly, we used 10 nM as the concentration for DHT treatment as a mode of activation of AR-mediated signalling in KGN cells in the current study. Pre-treatment with the AR antagonist flutamide (5 μM, 24 h) diminished the increased levels of FHL2 and AR induced by

DHT (Fig. 5e). These data indicate that the upregulation of FHL2 may result from AR-mediated androgen actions in PCOS.

3.6. Ovulatory dysfunction in rats due to FHL2 overexpression following intraovarian lentivirus injection

Given our findings of higher FHL2 expression in hGCs from patients with PCOS along with the in vitro data, we speculated that elevated FHL2 expression contributes to ovulatory dysfunction in PCOS. To further explore the role of FHL2 in regulating ovulation in vivo, FHL2-overexpressing rat ovaries were established via the intrabursal injection of lentivirus vectors [19,45−48]. One week after lentiviral injection, we induced superovulation. To confirm the data in vitro, we examined the expression pattern of FHL2, AR, C/EBPβ, COX2 and HAS2 at 0, 4 and 16 h after hCG treatment using control rat ovaries, which displayed similar expression trend to those of hCG-induced expression pattern in hGCs and FSK-induced expression trend in KGN cells (Figs. 2e, S2 and S4).

The efficiency of lentivirus-mediated FHL2 overexpression was examined in rat ovaries at each time point (Fig. 6a). We found no differences in body weight and ovarian weight between the FHL2-overexpressing and control groups (Fig. 6c). We examined serum progesterone levels at 16 h after hCG treatment, which were prominently lower in the FHL2 overexpression group than those in control group (Fig. 6b). Remarkably, the FHL2-overexpressing group displayed lower numbers of oocytes retrieved per ovary (11·10 $\pm$ 1·73 oocytes) than the control group (21·56 $\pm$ 2·59 oocytes) (Fig. 6d,f). Moreover, the rate of MII oocytes in the retrieved oocytes significantly decreased in the FHL2 overexpression group (Fig. 6e and f). We used HE staining to examine the ovarian morphology at 16 h after hCG treatment, and more large antral follicles and fewer corpora lutea were observed in the overexpression group than in the control group (Fig. 6h, S6). At 4 h after hCG treatment, a very early stage for cumulus expansion, we did not see the obvious difference between the two groups, both of which displayed a relatively low scale of the cumulus expansion (Fig. 6g). At 48 h after PMSG stimulation, we did not detect abnormal follicle development in either group (Fig. S5).

Moreover, we examined the expression of ovulation-related genes at 4 h after hCG treatment, which is a pivotal time point for LH surge to trigger ovulatory process. The results indicated that mRNA and protein levels of C/EBPβ, COX2 and HAS2 evidently decreased in the FHL2 overexpression group similar to phosphorylated ERK1/2 levels (Fig. 6i,j). These data further confirm that FHL2 can inhibit ovulation by suppressing essential ovulatory genes.

3.7. Effects of 3-week FHL2 overexpression in rat ovaries

Because 1-week of FHL2 overexpression in rat ovaries cause an impaired superovulatory response, we considered whether long-term FHL2 overexpression in rat ovaries can induce phenotypes similar to those of PCOS rat models [51]. We found that the FHL2 overexpression group displayed irregular oestrous cycles (Fig. 7a), and there were no differences in body and ovarian weight between the two groups (Fig. 7b). Notably, we found more preantral follicles, small antral follicles and cystic follicles, whereas fewer corpora lutea in the FHL2 overexpression group than in the control group (Fig. 7d, S7). Moreover, we detected decreased serum progesterone levels in the FHL2 overexpression group (Fig. 7c), which was consistent with the findings of ovulatory dysfunction. Our results suggested that 3 weeks of FHL2 overexpression following lentivirus vector implantation in rat ovaries can lead to acyclicity, PCOM, which were similar to the phenotypes of PCOS rat models. Furthermore, we also found that mRNA and protein levels of C/EBPβ, COX2 and HAS2, as well as protein expression of phosphorylated ERK1/2 profoundly decreased in the FHL2 overexpression group (Fig. 7e,f).
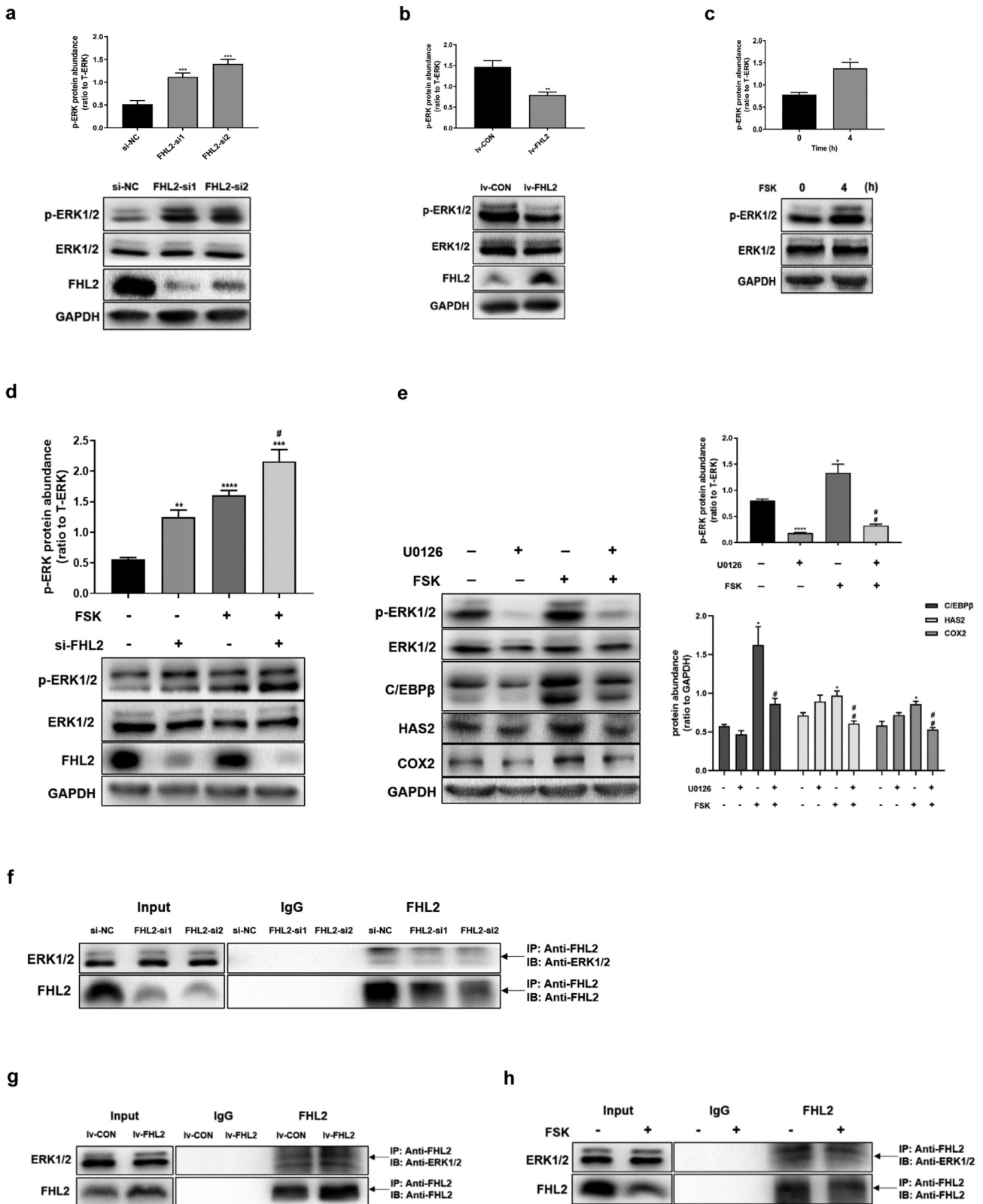
Fig. 4. Inhibition of ERK1/2 phosphorylation by FHL2 interacting with ERK1/2 and the role of ERK signalling in regulating ovulation-related genes in KGN cells. (a) Effect of siRNA-mediated FHL2 knockdown on the phosphorylation of ERK1/2. (b) Effect of FHL2 overexpression on the phosphorylation of ERK1/2. (c) Induction on the phosphorylation of ERK1/2 by FSK (10 μM, 4 h). (d) Effect of FSK (10 μM, 4 h) on the phosphorylation of ERK1/2 with or without FHL2 knockdown in KGN cells. (e) Effects of FSK (10 μM, 4 h) on ERK1/2 phosphorylation, C/EBPβ, HAS2 and COX2, in the presence and absence of inhibitor for ERK1/2 (U0126, 10 μM). (f-h) The FHL2-ERK1/2 interaction was examined in KGN cells by immunoprecipitation of FHL2 from whole-cell lysates followed by immunoblotting for ERK1/2 and FHL2. FHL2-ERK1/2 interaction was detected after siRNA-mediated FHL2 knockdown (f), stable transfection mediated by FHL2 lentivirus or control vectors (g), and treatment with FSK (10 μM, 4 h) (h), respectively. Representative blots are shown and the data are means ± SEM from 3 to 5 experiments. $^*P < 0.05$, $^{**}P < 0.01$, $^{***}P < 0.001$, $^{****}P < 0.0001$ vs. controls; $^{\#}P < 0.05$, $^{\#\#}P < 0.01$ vs. FSK.
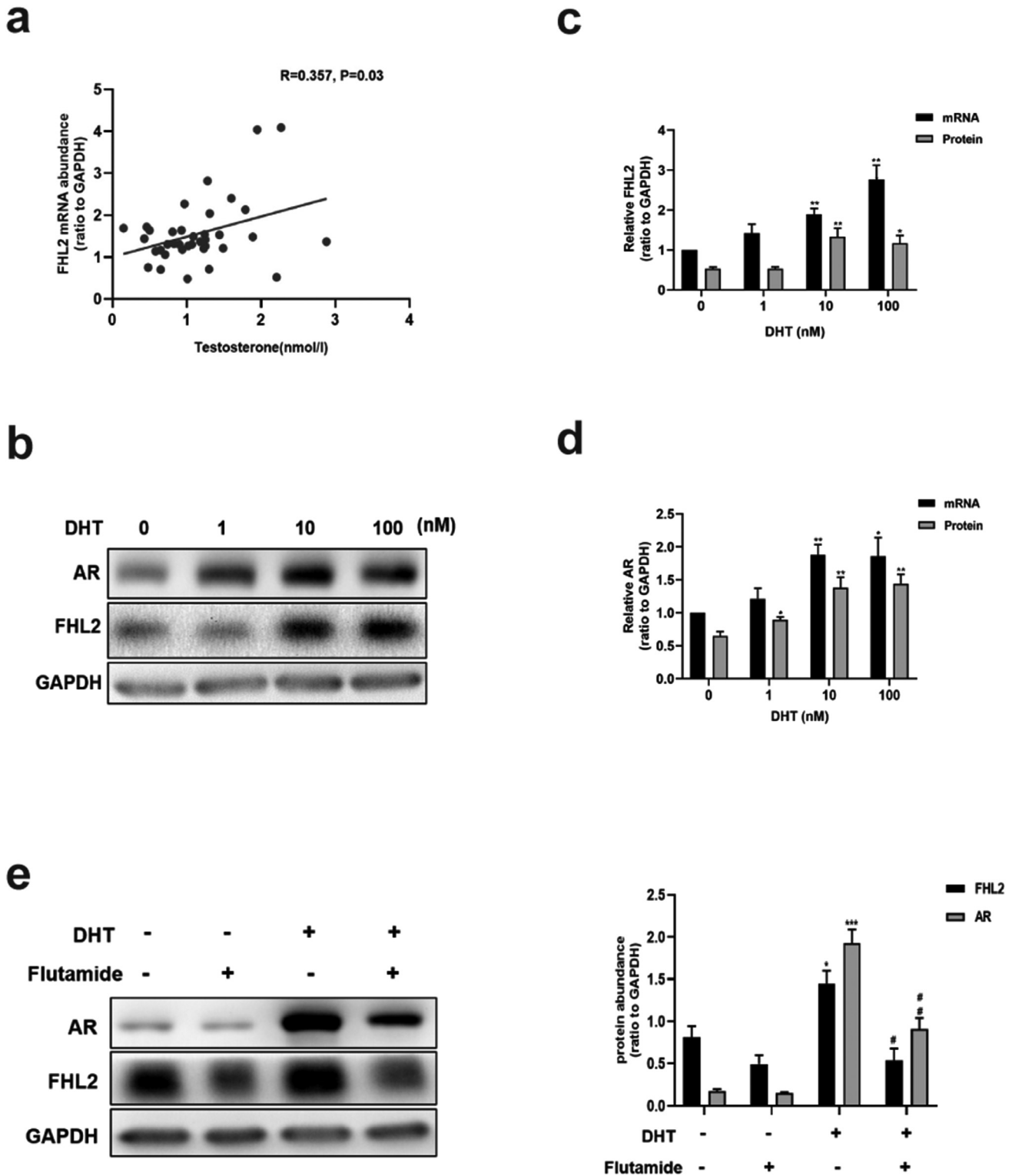
Fig. 5. Correlation between serum testosterone level and FHL2 abundance in hGCs from patients with PCOS and DHT-induced upregulation of FHL2 mediated by AR in KGN cells. (a) Spearman correlation analysis between FHL2 mRNA abundance in hGCs and basal serum testosterone level from patients with PCOS ($n = 37$). (b-d) Effects of various concentrations of DHT ($1-100$ nM, 24 h) on protein and mRNA levels of FHL2 and AR in KGN cells. (e) Effects of DHT (10 nM, 24 h) on protein levels of FHL2 and AR in the presence or absence of flutamide (an androgen receptor inhibitor, 5 μM, pretreated for 24 h). Representative blots are shown and the data are means $\pm$ SEM from 3 to 5 experiments. $^*P < 0.05$, $^{**}P < 0.01$, $^{***}P < 0.001$ vs. controls; $^{\#}P < 0.05$, $^{\#\#}P < 0.01$ vs. DHT.

4. Discussion

PCOS is the primary cause of anovulatory sub-fertility [5]. However, the mechanism underlying anovulation in PCOS remains unclear, and evidence suggests that aberrant follicular development

and terminal maturation of pre-ovulatory follicles, consequently lead to ovulatory dysfunction in patients with PCOS [5]. Although patients with PCOS undergoing IVF are typically characterised by an increased number of oocytes, the oocytes are often of poor quality, leading to lower fertilisation, cleavage, and implantation rates and a higher
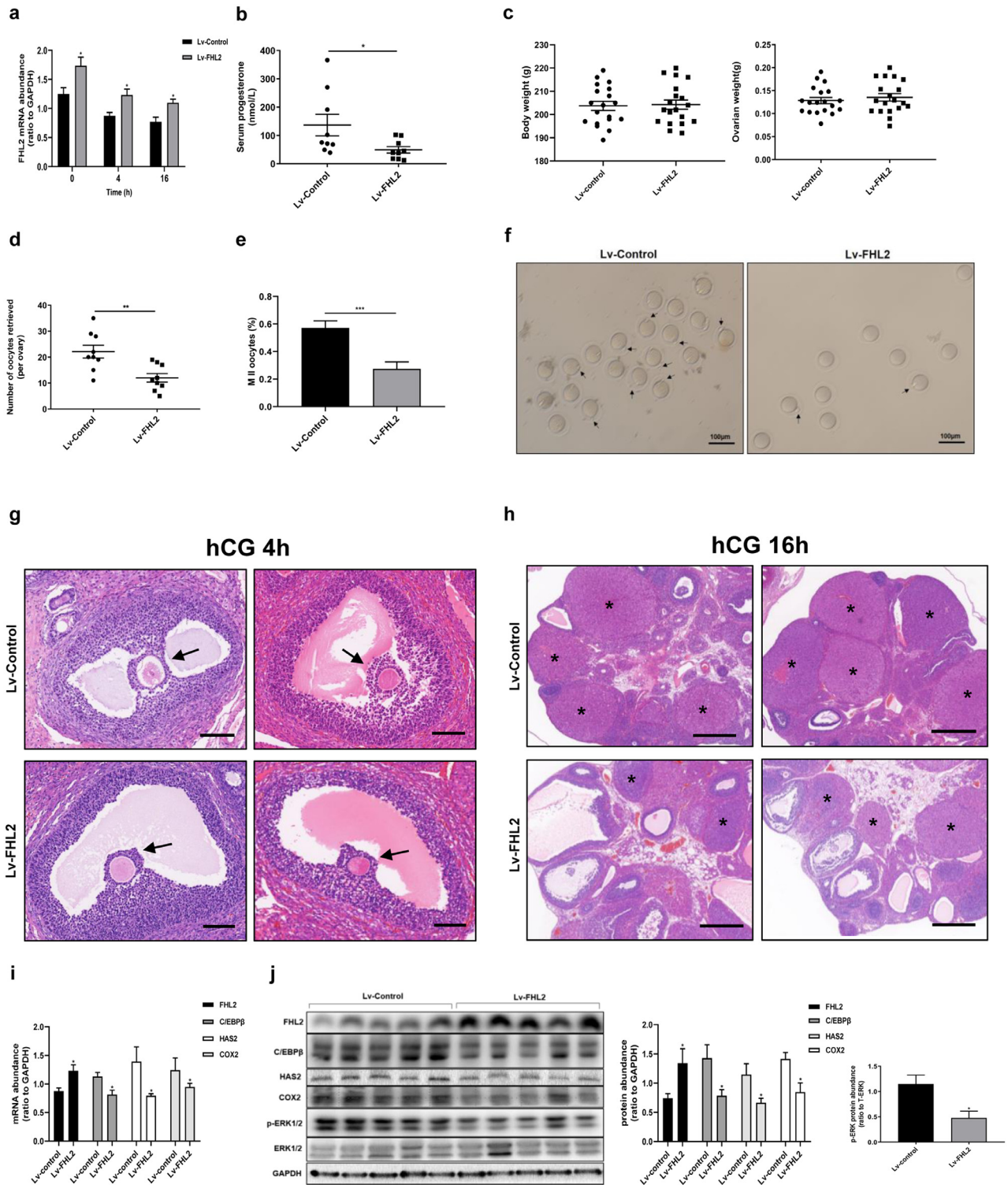
Fig. 6. Ovulatory dysfunction in rats due to FHL2 overexpression mediated by lentivirus vectors. (a) mRNA abundance of FHL2 in rat ovaries examined in rat ovaries at 0, 4 and 16 h after hCG triggering. (b) Serum progesterone levels after hCG 16 h detected by ELISA analysis (n = 9 for each group). (c) Body weight (left) and ovarian weight (right) of rats. (d) Numbers of retrieved oocytes per ovary (n = 9 for each group). (e) Ratio of MII oocytes. (f) Representative images of oocytes retrieved per ovary. Black arrows indicate MII oocytes. (g) Ovarian morphology of rats injected with control vector (above) or FHL2 lentivirus vector (below), followed by superovulation (PMSG 48 h + hCG 4 h) (n = 5 for each group). Black arrow indicates cumulus−oocyte complex. Scale bar, 100 μm. (h) Ovarian morphology of rats injected with control vector (above) or FHL2 lentivirus vector (below), followed by superovulation (PMSG 48 h + hCG16 h). Asterisk stands for corpus luteum. Scale bar, 500 μm. (i) At 4 h after hCG, mRNA levels of FHL2, C/EBPβ, HAS2 and COX2 were analysed from ovaries of two groups (n = 5 for each group). (j) At 4 h after hCG, protein levels of FHL2, C/EBPβ, HAS2, COX2, and the phosphorylation of ERK1/2 were analysed from ovaries of two groups. The data are means ± SEM. *$P < 0.05$, **$P < 0.01$, ***$P < 0.001$ vs. the control group.

miscarriage rate [53−56]. The underlying mechanism for this observation remains to be elucidated.

Based on published microarray data and using bioinformatics, we revealed that FHL2 may regulate these differentially expressed genes in GCs or ovarian tissues in patients with PCOS [16−18]. Indeed, the abundance of FHL2 was higher the PCOS group than in the non-PCOS group. Although the expression of FHL2 has been detected predominantly in the GCs, oocytes and theca cells [22,33], its function in the
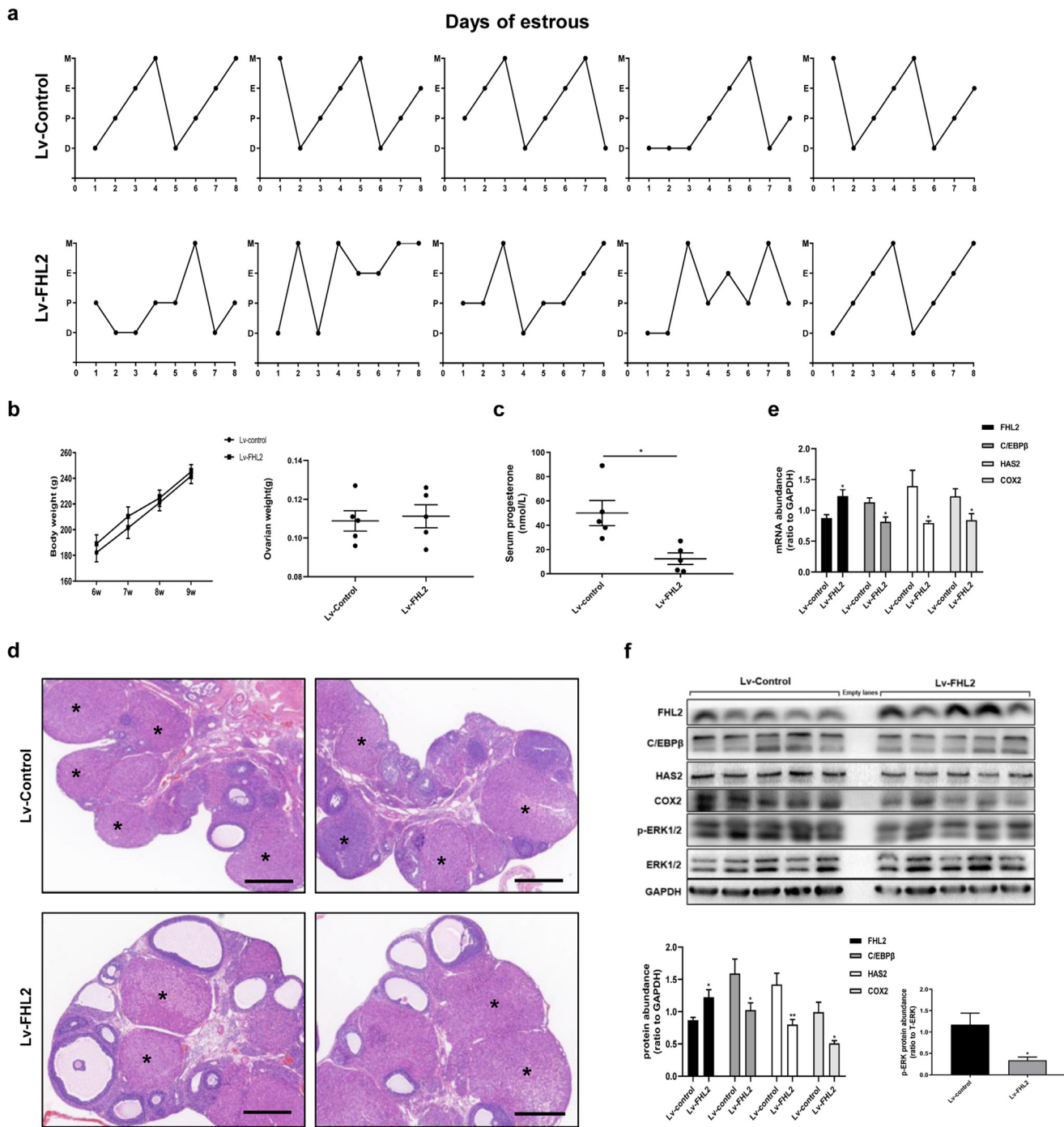
Fig. 7. Effects of 3-week FHL2 overexpression in rat ovaries mediated by lentivirus vectors. (a) Estrous cycles were detected in rats injected with control vector (above) or FHL2 lentivirus vector (below). D, dioestrus; P, proestrus; E, oestrus; M, metestrus. (b) Body weight (left) and ovarian weight (right) of rats. (c) Serum Progesterone levels detected by ELISA analysis. (d) Ovarian morphology of rats injected with control vector (above) or FHL2 lentivirus vector (below). Asterisk stands for corpus luteum. Scale bar, 500 μm. (e) mRNA levels of FHL2, C/EBPβ, HAS2 and COX2 from ovaries of two groups. (f) Protein levels of FHL2, C/EBPβ, HAS2, COX2, and the phosphorylation of ERK1/2 from ovaries of two groups. n = 5 for each group. The data are means ± SEM. $^{*}P < 0.05$, $^{**}P < 0.01$ vs. the control group.

ovaries has not been fully established. In the current study, we focused on its role in ovulation. LH surge-induced FHL2 downregulation was detected both *in vitro* and *in vivo*, suggesting its likely importance in regulating ovulatory process.

In vitro experiments illustrated that *FHL2* could negatively regulate ovulation-related genes including *C/EBPβ, COX2* and *HAS2*. It has been demonstrated that *C/EBPβ*-deficient mice are sub-fertile, and they display impaired COC expansion and absence of corpora lutea, leading to ovulatory dysfunction [15,57]. *C/EBPα*-deficient mice exhibit normal fertility, nevertheless, *C/EBPα/β*$^{gc-/-}$ double-mutant

mice are anovulatory [15,46]. Gene expression profiling provides critical data for identifying which genes regulated by the LH activation of ERK1/2 [14] are also targets of C/EBPα/β [15]. In particular, a subset (19%) of genes was found to be regulated similarly in the GCs of *Erk1/2*$^{gc-/-}$ and *C/EBPα/β*$^{gc-/-}$ mice at 4 h after hCG treatment, including COX2 and HAS2 [14,15,57], and their expression was partially impeded by siRNA-mediated *C/EBPβ* depletion in KGN cells (Fig. S1).

Previous research suggested that AR activity can suppress the expression of C/EBPβ, which was a direct AR transcriptional repression target in prostate cancer cells [39]. In recent years, *in vitro* studies and

in vivo animal models revealed several intra-ovarian pathways which are responsive to elevated androgen exposure, and AR-mediated androgen actions play a key role in the development of PCOS phenotypes [58−62]. Loss of AR signalling protects female mice against the induction of PCOS features by hyperandrogenism [63,64], including anovulation; however, the underlying mechanisms remain to be fully characterised. In the current study, we detected elevated AR abundance in hGCs from patients with PCOS and inhibition effect on the expression of C/EBPβ, COX2 and HAS2 by AR in KGN cells. Furthermore, we demonstrated that DHT, as an activator of AR [44], increased the enrichment of AR at the C/EBPβ promoter, suggesting that AR inhibited C/EBPβ expression by binding to its promoter region.

To explore the molecular mechanism by which upregulated FHL2 suppresses ovulation-related genes, we hypothesised that because FHL2 cannot bind to DNA, it acts as a mediator via protein−protein interactions and functions as a transcriptional co-regulator to regulate the expression of ovulation-related genes [20,21]. In this study, we detected an interaction between FHL2 and AR, and FHL2 overexpression increased the binding of AR to the C/EBPβ promoter. Moreover, the inhibition of C/EBPβ by FHL2 overexpression was rescued by AR depletion in KGN cells. Overall, these data suggest that the downregulated C/EBPβ expression observed in patients with PCOS may be partially explained by the indirect inhibitory effects of FHL2 via its interaction with AR at the C/EBPβ promoter.

It has been well established that the ERK pathway plays pivotal roles in ovulation [10−13]. Previous studies documented that ERK1/2 controls the expression of many genes rapidly induced (within 4 h) by the LH surge in the GCs of pre-ovulatory follicles [14]. In this study, we found that pre-treatment with an inhibitor of ERK signalling (U0126) effectively abolished the FSK-mimicked LH surge-induced upregulation of C/EBPβ, COX2 and HAS2. Unexpectedly, we detected that FHL2 inhibited the activation of ERK signalling by binding to ERK1/2. This indicates that FHL2 could function as a repressor of ERK1/2 to suppress ovulation-related genes. These data verified previous findings that genes involved in MAPK/ERK signalling pathways may influence the function of GCs in PCOS, as well as data that phosphorylated ERK1/2 expression decreased in GCs from patients with PCOS [65,66].

Furthermore, we found that the abundance of FHL2 in the GCs of patients with PCOS was positively correlated with basal serum T levels. Several lines of evidence have confirmed the essential role of androgens in the development of PCOS [67]. Our results demonstrated that DHT increased the expression of FHL2, which was mediated by AR signalling. Moreover, DHT enhanced the interaction between FHL2 and AR. These data indicate that FHL2 may relate to AR-mediated androgen actions in PCOS. However, we could not clarify the mechanism connecting the increased FHL2 levels in GCs from patients with PCOS and androgen excess due to the unavailability of theca cells, which should be resolved in the future study.

The contribution of FHL2 to ovulation was further investigated *in vivo* by intrabursally injecting FHL2-overexpressing lentivirus into rat ovaries. In this study, we found that FHL2 overexpression in rat ovaries led to the inhibition of ovulation-related genes, including phospho-ERK1/2, C/EBPβ, COX2, and HAS2, which may jeopardise COC expansion, oocyte maturation, and follicular rupture [14,15]. Indeed, after 1 week of modelling followed by superovulation, FHL2 overexpression rats displayed significantly decreased ovulation efficiency and MII oocyte rate. Following 3 weeks of modelling, we detected that FHL2 overexpression group displayed acyclicity and PCOM, which were similar to the phenotypes of PCOS rat models observed previously in our laboratory [19,68]. All of these clues indicate that FHL2 may play a role in the development of the ovarian features of PCOS. These data collectively support the pivotal role of FHL2 in suppressing ovulation, which confirm the molecular mechanisms identified *in vitro*. However, there were discrepancies between the response of FHL2-overexpressing rats to superovulation and that of

PCOS patients, which could be overcome by gonadotropin stimulation. PCOS is a complex disease and it involves multiple factors in the pathogenesis of PCOS, and the role of FHL2 may be only involved in part of the development of ovarian features of PCOS.

On the basis of our findings and the already known ovulatory process activated by LH signalling, we generated a diagram which presents the postulated roles of FHL2 in inhibiting ovulation in the development of ovulatory dysfunction in PCOS (Fig. 8). According to this scheme, it is hypothesised that the profound effects of aberrant FHL2 on AR signalling and ERK pathway may result in the blockade of ovulation in PCOS; meanwhile, AR-mediated androgen (DHT) actions may stimulate FHL2 upregulation. Further studies are needed to confirm our hypothesis.

Among the limitations of our study is the fact that we assessed only the numbers of oocytes retrieved to evaluate the role of FHL2 in ovulation. However, sub-fertility in patients with PCOS could be attributed to both a failure to release mature oocytes and follicular growth-associated obstacles which we could not explore in-depth in rat ovaries due to species differences and technical challenges. Second, there were technical difficulties in maintaining sufficient numbers of hGCs. And there was few evidence for the similarity and difference between the human luteinized GCs and non-luteinized GCs responding to various stimulation *in vitro* experiment [69,70]. Because of the complexity of FHL2-related pathway studies, we decided to perform most of our *in vitro* experiments using KGN cells, a human granulosa-like tumour cell line [71]. Another limitation of our study was the reliance on human cell cultures and a rodent animal model. Accordingly, our observations must be validated in a primate model and in the human context. We assume that conditional knockout or gain-of-function of FHL2 in GCs or theca cells in animal models are needed to further confirm the specific role of FHL2 in the reproductive system.
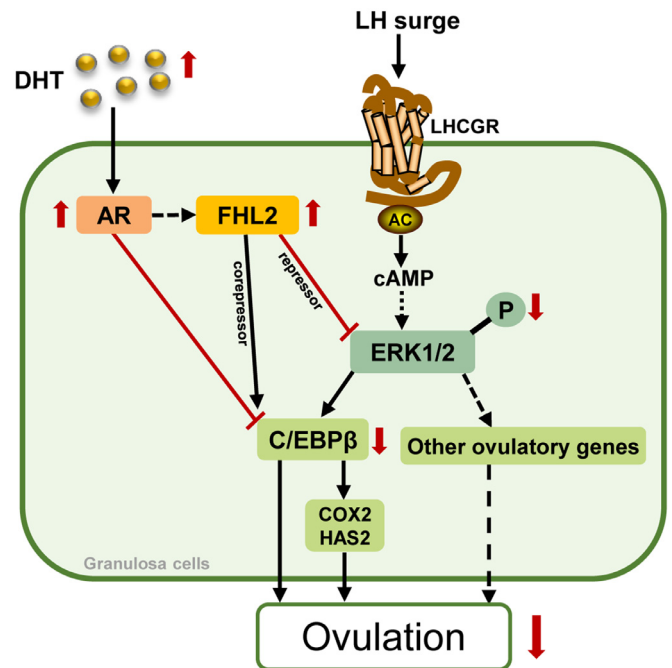
Fig. 8. Modelling the roles of FHL2 in inhibiting ovulation in PCOS.

All of the events of ovulation are triggered by LH surge that result in the activation of LHCGR−adenylyl cyclase (AC)−cAMP in GCs. Activation of cAMP in GCs leading to activation of ERK1/2 cascade involved in oocyte maturation, cumulus expansion and follicle rupture. In PCOS, elevated FHL2 expression leads to blockade of ovulation by: (i) interacting with AR to act as its co-repressor to inhibit C/EBPβ expression; (ii) binding to ERK1/2 to inhibit its phosphorylation, inducing further suppression of C/EBPβ and other ovulatory genes. Moreover, androgen (DHT)-induced upregulation of FHL2 is mediated by AR.

In conclusion, our data demonstrate that FHL2 may play an important role in the development of ovulatory dysfunction in PCOS and that its upregulation is associated with hyperandrogenism. The upregulated FHL2 could inhibit ovulation by targeting AR and ERK signalling pathways. Moreover, AR-mediated androgen actions could induce FHL2 upregulation. Our findings may provide a potential therapeutic approach for the treatment of PCOS, and inhibition of abnormally elevated FHL2 expression in combination with assisted reproductive technology may be a promising molecular strategy for treating ovulatory dysfunction in PCOS.

Declaration of Competing Interest

The authors declare that they have no competing interests.

Author contributions

Ruiqiong Zhou, Shang Li, Jiansheng Liu, Yun Sun, Zi-Jiang Chen, Weiping Li and Yanzhi Du designed the study. Ruiqiong Zhou and Hasiximuke Wu collected patient specimens and related information. Ruiqiong Zhou, Shang Li, Jiansheng Liu, Guangxin Yao and Yanzhi Du contributed to conducting the experiments and analysing the data. Ruiqiong Zhou and Yanzhi Du drafted and revised the paper. All authors reviewed the results and approved the final version of the manuscript.

Supplementary materials

Supplementary material associated with this article can be found in the online version at doi:10.1016/j.ebiom.2020.102635.

References

[1] Azziz R, Carmina E, Dewailly D, Diamanti-Kandarakis E, Escobar-Morreale HF, Futterweit W, et al. The androgen excess and PCOS society criteria for the polycystic ovary syndrome: the complete task force report. Fertil Steril. 2009;91(2):456–88.

[2] Wen L, Liu Q, Xu J, Liu X, Shi C, Yang Z, et al. Recent advances in mammalian reproductive biology. Sci China Life Sci 2019. doi: 10.1007/s11427-019-1572-7.

[3] Goodarzi MO, Dumesic DA, Chazenbalk G, Azziz R. Polycystic ovary syndrome: etiology, pathogenesis and diagnosis. Nat Rev Endocrinol 2011;7(4):219–31.

[4] Azziz R, Woods KS, Reyna R, Key TJ, Knochenhauer ES, Yildiz BO. The prevalence and features of the polycystic ovary syndrome in an unselected population. J Clin Endocrinol Metab. 2004;89(6):2745–9.

[5] Azziz R, Carmina E, Chen Z, Dunaif A, Laven JS, Legro RS, et al. Polycystic ovary syndrome. Nat Rev Dis Primers 2016;2:16057.

[6] Gorry A, White DM, Franks S. Infertility in polycystic ovary syndrome: focus on low-dose gonadotropin treatment. Endocrine 2006;30(1):27–33.

[7] Hughesdon PE. Morphology and morphogenesis of the Stein-Leventhal ovary and of so-called "hyperthecosis". Obstet Gynecol Surv. 1982;37(2):59–77.

[8] Franks S, Mason H, Willis D. Follicular dynamics in the polycystic ovary syndrome. Mol Cell Endocrinol. 2000;163(1−2):49–52.

[9] Richards JS, Ascoli M. Endocrine, paracrine, and autocrine signaling pathways that regulate ovulation. Trends Endocrinol Metab 2018;29(5):313–25.

[10] Shimada M, Hernandez-Gonzalez I, Gonzalez-Robayna I, Richards JS. Paracrine and autocrine regulation of epidermal growth factor-like factors in cumulus oocyte complexes and granulosa cells: key roles for prostaglandin synthase 2 and progesterone receptor. Mol Endocrinol 2006;20(6):1352–65.

[11] Conti M, Hsieh M, Park JY, Su YQ. Role of the epidermal growth factor network in ovarian follicles. Mol Endocrinol 2006;20(4):715–23.

[12] Su YQ, Wigglesworth K, Pendola FL, O'Brien MJ, Eppig JJ. Mitogen-activated protein kinase activity in cumulus cells is essential for gonadotropin-induced oocyte meiotic resumption and cumulus expansion in the mouse. Endocrinology 2002;143(6):2221–32.

[13] Park JY, Su YQ, Ariga M, Law E, Jin SL, Conti M. EGF-like growth factors as mediators of LH action in the ovulatory follicle. Science 2004;303(5658):682–4.

[14] Fan HY, Liu Z, Shimada M, Sterneck E, Johnson PF, Hedrick SM, et al. MAPK3/1 (ERK1/2) in ovarian granulosa cells are essential for female fertility. Science 2009;324(5929):938–41.

[15] Fan HY, Liu Z, Johnson PF, Richards JS. CCAAT/enhancer-binding proteins (C/EBP)-alpha and -beta are essential for ovulation, luteinization, and the expression of key target genes. Mol Endocrinol 2011;25(2):253–68.

[16] Kaur S, Archer KJ, Devi MG, Kriplani A, Strauss 3rd. JF, Singh R. Differential gene expression in granulosa cells from polycystic ovary syndrome patients with and without insulin resistance: identification of susceptibility gene sets through network analysis. J Clin Endocrinol Metab 2012;97(10):E2016–21.

[17] Kenigsberg S, Bentov Y, Chalifa-Caspi V, Potashnik G, Ofir R, Birk OS. Gene expression microarray profiles of cumulus cells in lean and overweight-obese polycystic ovary syndrome patients. Mol Hum Reprod 2009;15(2):89–103.

[18] Jansen E, Laven JS, Dommerholt HB, Polman J, van Rijt C, van den Hurk C, et al. Abnormal gene expression profiles in human ovaries from polycystic ovary syndrome patients. Mol Endocrinol 2004;18(12):3050–63.

[19] Li S, Zhai J, Liu J, Di F, Sun Y, Li W, et al. Erythropoietin-producing hepatocellular A7 triggering ovulation indicates a potential beneficial role for polycystic ovary syndrome. EBioMedicine 2018;36:539–52.

[20] Sanchez-Garcia I, Rabbitts TH. The Lim domain: a new structural motif found in zinc-finger-like proteins. Trends Genet 1994;10(9):315–20.

[21] Chu PH, Ruiz-Lozano P, Zhou Q, Cai C, Chen J. Expression patterns of FHL/slim family members suggest important functional roles in skeletal muscle and cardiovascular system. Mech Dev 2000;95(1−2):259–65.

[22] Fimia GM, De Cesare D, Sassone-Corsi P. A family of LIM-only transcriptional coactivators: tissue-specific expression and selective activation of Creb and Crem. Mol Cell Biol 2000;20(22):8613–22.

[23] Genini M, Schwalbe P, Scholl FA, Remppis A, Mattei MG, Schafer BW. Subtractive cloning and characterization of DRAL, a novel LIM-domain protein down-regulated in rhabdomyosarcoma. DNA Cell Biol 1997;16(4):433–42.

[24] Matulis CK, Mayo KE. The Lim domain protein FHL2 interacts with the NR5A family of nuclear receptors and Creb to activate the inhibin-alpha subunit gene in ovarian granulosa cells. Mol Endocrinol 2012;26(8):1278–90.

[25] Muller JM, Metzger E, Greschik H, Bosserhoff AK, Mercep L, Buettner R, et al. The transcriptional coactivator FHL2 transmits rho signals from the cell membrane into the nucleus. Embo J 2002;21(4):736–48.

[26] Labalette C, Nouet Y, Sobczak-Thepot J, Armengol C, Levillayer F, Gendron MC, et al. The LIM-only protein FHL2 regulates cyclin D1 expression and cell proliferation. J Biol Chem 2008;283(22):15201–8.

[27] Wang J, Yang Y, Xia HH, Gu Q, Lin MC, Jiang B, et al. Suppression of FHL2 expression induces cell differentiation and inhibits gastric and colon carcinogenesis. Gastroenterology 2007;132(3):1066–76.

[28] Gunther T, Poli C, Muller JM, Catala-Lehnen P, Schinke T, Yin N, et al. Fhl2 deficiency results in osteopenia due to decreased activity of osteoblasts. Embo J 2005;24(17):3049–56.

[29] Govoni KE, Baylink DJ, Chen J, Mohan S. Disruption of four-and-a-half lim 2 decreases bone mineral content and bone mineral density in femur and tibia bones of female mice. Calcif Tissue Int 2006;79(2):112–7.

[30] Kong Y, Shelton JM, Rothermel B, Li X, Richardson JA, Bassel-Duby R, et al. Cardiac-specific Lim protein FHL2 modifies the hypertrophic response to beta-adrenergic stimulation. Circulation 2001;103(22):2731–8.

[31] Purcell NH, Darwis D, Bueno OF, Muller JM, Schule R, Molkentin JD. Extracellular signal-regulated kinase 2 interacts with and is negatively regulated by the LIM-only protein FHL2 in cardiomyocytes. Mol Cell Biol 2004;24(3):1081–95.

[32] Chu PH, Bardwell WM, Gu Y, Ross Jr. J, Chen J. FHL2 (SLIM3) is not essential for cardiac development and function. Mol Cell Biol 2000;20(20):7460–2.

[33] Du X, Hublitz P, Gunther T, Wilhelm D, Englert C, Schule R. The LIM-only coactivator FHL2 modulates WT1 transcriptional activity during gonadal differentiation. Biochim Biophys Acta 2002;1577(1):93–101.

[34] Nisenblat V, Norman RJ. Androgens and polycystic ovary syndrome. Curr Opin Endocrinol Diabetes Obes 2009;16(3):224–31.

[35] Baculescu N. The role of androgen receptor activity mediated by the CAG repeat polymorphism in the pathogenesis of PCOS. J Med Life 2013;6(1):18–25.

[36] Wang F, Pan J, Liu Y, Meng Q, Lv P, Qu F, et al. Alternative splicing of the androgen receptor in polycystic ovary syndrome. Proc Natl Acad Sci U S A 2015;112(15):4743–8.

[37] Kollara A, Brown TJ. Four and a half lim domain 2 alters the impact of aryl hydrocarbon receptor on androgen receptor transcriptional activity. J Steroid Biochem Mol Biol 2010;118(1−2):51–8.

[38] Muller JM, Isele U, Metzger E, Rempel A, Moser M, Pscherer A, et al. FHL2, a novel tissue-specific coactivator of the androgen receptor. Embo J 2000;19(3):359–69.

[39] Barakat DJ, Zhang J, Barberi T, Denmeade SR, Friedman AD, Paz-Priel I. CCAAT/ Enhancer binding protein beta controls androgen-deprivation-induced senescence in prostate cancer cells. Oncogene 2015;34(48):5912–22.

[40] Revised 2003 consensus on diagnostic criteria and long-term health risks related to polycystic ovary syndrome (PCOS). Hum Reprod 2004;19(1):41–7.

[41] Cheng JC, Fang L, Chang HM, Sun YP, Leung PC. hCG-induced sprouty2 mediates amphiregulin-stimulated COX-2/PGE2 up-regulation in human granulosa cells: a potential mechanism for the OHSS. Sci Rep 2016;6:31675.

[42] Morris JK, Richards JS. Hormone induction of luteinization and prostaglandin endoperoxide synthase-2 involves multiple cellular signaling pathways. Endocrinology 1993;133(2):770–9.

[43] Yerushalmi GM, Markman S, Yung Y, Maman E, Aviel-Ronen S, Orvieto R, et al. The prostaglandin transporter (PGT) as a potential mediator of ovulation. Sci Transl Med 2016;8(338):338ra68.

[44] Li D, Zhou W, Pang J, Tang Q, Zhong B, Shen C, et al. A magic drug target: androgen receptor. Med Res Rev 2019;39(5):1485–514.

[45] Giry-Laterriere M, Verhoeyen E, Salmon P. Lentiviral vectors. Methods Mol Biol 2011;737:183–209.

[46] Piontkewitz Y, Enerback S, Hedin L. Expression of CCAAT enhancer binding protein-alpha (C/EBP alpha) in the rat ovary: implications for follicular development and ovulation. Dev Biol 1996;179(1):288–96.

[47] Sugiura K, Su YQ, Eppig JJ. Targeted suppression of HAS2 mRNA in mouse cumulus cell-oocyte complexes by adenovirus-mediated short-hairpin RNA expression. Mol Reprod Dev 2009;76(6):537–47.

[48] Di F, Liu J, Li S, Yao G, Hong Y, Chen ZJ, et al. ATF4 contributes to ovulation via regulating COX2/PGE2 expression: a potential role of ATF4 in PCOS. Front Endocrinol 2018;9:669.

[49] Popova E, Krivokharchenko A, Ganten D, Bader M. Comparison between PMSG- and FSH-induced superovulation for the generation of transgenic rats. Mol Reprod Dev 2002;63(2):177–82.

[50] Dou YD, Zhao H, Huang T, Zhao SG, Liu XM, Yu XC, et al. STMN1 promotes progesterone production via star up-regulation in mouse granulosa cells. Sci Rep 2016;6:26691.

[51] Caldwell AS, Middleton LJ, Jimenez M, Desai R, McMahon AC, Allan CM, et al. Characterization of reproductive, metabolic, and endocrine features of polycystic ovary syndrome in female hyperandrogenic mouse models. Endocrinology 2014;155(8):3146–59.

[52] Caldwell ASL, Edwards MC, Desai R, Jimenez M, Gilchrist RB, Handelsman DJ, et al. Neuroendocrine androgen action is a key extraovarian mediator in the development of polycystic ovary syndrome. Proc Natl Acad Sci USA 2017;114 (16):E3334–e43.

[53] Qiao J, Feng HL. Extra- and intra-ovarian factors in polycystic ovary syndrome: impact on oocyte maturation and embryo developmental competence. Hum Reprod Update 2011;17(1):17–33.

[54] Palomba S, de Wilde MA, Falbo A, Koster MP, La Sala GB, Fauser BC. Pregnancy complications in women with polycystic ovary syndrome. Hum Reprod Update 2015;21(5):575–92.

[55] Sahu B, Ozturk O, Ranierri M, Serhal P. Comparison of oocyte quality and intracytoplasmic sperm injection outcome in women with isolated polycystic ovaries or polycystic ovarian syndrome. Arch Gynecol Obstet 2008;277(3):239–44.

[56] Mulders AG, Laven JS, Imani B, Eijkemans MJ, Fauser BC. IVF outcome in anovulatory infertility (WHO group 2)−including polycystic ovary syndrome−following previous unsuccessful ovulation induction. Reprod Biomed Online 2003;7 (1):50–8.

[57] Sterneck E, Tessarollo L, Johnson PF. An essential role for C/EBPbeta in female reproduction. Genes Dev. 1997;11(17):2153–62.

[58] Walters KA, Allan CM, Handelsman DJ. Rodent models for human polycystic ovary syndrome. Biol Reprod. 2012;86(5):149. 1-12.

[59] Padmanabhan V, Veiga-Lopez A. Sheep models of polycystic ovary syndrome phenotype. Mol Cell Endocrinol 2013;373(1−2):8–20.

[60] Wu CH, Yang JG, Yang JJ, Lin YM, Tsai HD, Lin CY, et al. Androgen excess down-regulates connexin43 in a human granulosa cell line. Fertil Steril 2010;94 (7):2938–41.

[61] Yang JL, Zhang CP, Li L, Huang L, Ji SY, Lu CL, et al. Testosterone induces redistribution of forkhead box-3a and down-regulation of growth and differentiation factor 9 messenger ribonucleic acid expression at early stage of mouse folliculogenesis. Endocrinology 2010;151(2):774–82.

[62] Hossain MM, Cao M, Wang Q, Kim JY, Schellander K, Tesfaye D, et al. Altered expression of miRNAs in a dihydrotestosterone-induced rat PCOS model. J Ovarian Res 2013;6(1):36.

[63] Caldwell AS, Eid S, Kay CR, Jimenez M, McMahon AC, Desai R, et al. Haplosufficient genomic androgen receptor signaling is adequate to protect female mice from induction of polycystic ovary syndrome features by prenatal hyperandrogenization. Endocrinology 2015;156(4):1441–52.

[64] Caldwell ASL, Edwards MC, Desai R, Jimenez M, Gilchrist RB, Handelsman DJ, et al. Neuroendocrine androgen action is a key extraovarian mediator in the development of polycystic ovary syndrome. Proc Natl Acad Sci U S A 2017;114(16): E3334–e43.

[65] Lan CW, Chen MJ, Tai KY, Yu DC, Yang YC, Jan PS, et al. Functional microarray analysis of differentially expressed genes in granulosa cells from women with polycystic ovary syndrome related to MAPK/ERK signaling. Sci Rep 2015;5: 14994.

[66] Nelson-Degrave VL, Wickenheisser JK, Hendricks KL, Asano T, Fujishiro M, Legro RS, et al. Alterations in mitogen-activated protein kinase kinase and extracellular regulated kinase signaling in theca cells contribute to excessive androgen production in polycystic ovary syndrome. Mol Endocrinol 2005;19(2):379–90.

[67] Walters KA. Role of androgens in normal and pathological ovarian function. Reproduction 2015;149(4):R193–218.

[68] Zhai J, Li S, Cheng X, Chen ZJ, Li W, Du Y. A candidate pathogenic gene, zinc finger gene 217 (ZNF217) may contribute to polycystic ovary syndrome through prostaglandin E2. Acta Obstet Gynecol Scand 2019.

[69] Lindeberg M, Carlström K, Ritvos O, Hovatta O. Gonadotrophin stimulation of non-luteinized granulosa cells increases steroid production and the expression of enzymes involved in estrogen and progesterone synthesis. Hum Reprod 2007;22 (2):401–6.

[70] Yerushalmi GM, Maman E, Yung Y, Kedem A, Hourvitz A. Molecular characterization of the human ovulatory cascade-lesson from the IVF/IVM model. J Assist Reprod Genet 2011;28(6):509–15.

[71] Nishi Y, Yanase T, Mu Y, Oba K, Ichino I, Saito M, et al. Establishment and characterization of a steroidogenic human granulosa-like tumor cell line, KGN, that expresses functional follicle-stimulating hormone receptor. Endocrinology 2001;142(1):437–45.